ELSEVIER

Surface Science 481 (2001) 13–24

SURFACE SCIENCE

www.elsevier.nl/locate/susc

Continuous and discontinuous transitions on 3D equilibrium crystal shapes: a new look at Pb and Au

A. Emundts [a], H.P. Bonzel [a,*], P. Wynblatt [b], K. Thürmer [c], J. Reutt-Robey [c], E.D. Williams [c]

[a] *Institut für Grenzflächenforschung und Vakuumphysik, Forschungszentrum Jülich, Postfach 1913, D-52425 Jülich, Germany*
[b] *Department of Materials Science and Engineering, Carnegie-Mellon University, Pittsburgh, PA 15213, USA*
[c] *Materials Research Science and Engineering Center, University of Maryland, College Park, MD 20742-4111, USA*

Received 6 November 2000; accepted for publication 3 April 2001

Abstract

Equilibrium crystal shapes exhibit flat facets and rough vicinal surfaces, with transitions between them being either continuous or discontinuous, the latter recognizable by a sharp edge. In general, mixed repulsive/attractive step–step interactions may lead to continuous or discontinuous facet-to-vicinal transitions. In can be shown that the contact angle at the facet for a discontinuous transition is directly related to the ratio of the step interaction strengths. Alternatively, surface reconstruction of facets can also be responsible for sharp edges at the facet boundary. In this case the contact angle is related to the difference between surface free energies of the reconstructed and unreconstructed facet as well as the corresponding difference of step interaction energies. Fitting the experimental shapes by theoretical expressions can be used to extract the relevant surface and step free energies and also step interaction energies. Experimental examples of Pb and Au equilibrium shapes are evaluated and discussed. Step free energies of vicinal Au(1 1 1) and Au(1 0 0) surfaces, evaluated by both models, are 30 and 10 meV/Å^2, respectively. © 2001 Elsevier Science B.V. All rights reserved.

Keywords: Equilibrium thermodynamics and statistical mechanics; Faceting; Surface energy; Surface structure, morphology, roughness, and topography; Vicinal single crystal surfaces; Scanning tunneling microscopy; Scanning electron microscopy (SEM)

1. Introduction

The theoretical and experimental study of the 3D equilibrium crystal shape of small crystallites has been of continuous interest over the past three decades [1–13] and has recently received new momentum through the application of high resolution scanning tunneling microscopy (STM) to the imaging of portions of nano- and micro-meter-sized crystals, supported on flat substrates [14–18]. An issue of particular interest has been the transition from atomically flat facets to rough vicinal surfaces [19]. These transitions may be continuous or discontinuous, equivalent to a smooth shape transition or the appearance of a sharp edge, corresponding to second and first order phase transitions, respectively [19–21]. The standard examples for these two cases seem to be Pb and Au equilibrium crystal shapes (ECSs) where the latter

* Corresponding author. Tel.: +49-2461-613270; fax: +49-2461-613907.
E-mail address: h.bonzel@fz-juelich.de (H.P. Bonzel).

0039-6028/01/$ - see front matter
PII: S0039-6028(01)01055-X

exhibits sharp edges at the (1 1 1) and (1 0 0) facet boundaries, at least at temperatures below 1123 K [5,9]. Such sharp edges have also been observed on cylindrically modulated (1 1 1) and (1 0 0) single crystal Au surfaces under quasi-steady-state conditions [22,23]. These observations are consistent with the behavior of flat Au single crystal vicinal surfaces near (1 1 1) or (1 0 0) orientations which have been shown to be unstable at elevated temperatures and to develop faceting [24–30].

There are two physical models that readily explain the appearance of sharp edges at low-index facets on the ECS. The first has a theoretical link to attractive next-nearest neighbor interactions [1,2] and accordingly, in the framework of a step interaction model, to attractive step–step interactions [3]. Hence step bunching on vicinal surfaces can be related to a long-range net attractive step interaction [31]. In the second model the reconstruction of low-index orientations, such as (1 1 1) and (1 0 0), plays an important role in that their surface free energies are lower than those of the unreconstructed terraces of the neighboring vicinal surfaces [32,33]. Due to this free energy difference, a sharp edge between the facet and vicinal surface on the ECS can appear. For the same reason facetting of flat vicinal surfaces is known to occur [30,34]. Such phenomena have been detected and widely investigated for Au [22,24,26–28,35–37] and Pt surfaces [38–40] but also for Si(1 1 1), for example [41–43]. In the present paper we will revisit the issue of smooth versus sharp edges, in connection with repulsive versus attractive step–step interactions as well as facet reconstruction. The main purpose will be the fitting of vicinal shapes, taken from the ECS, with analytical expressions of the surface free energy and the evaluation of relative step free energies, both for smooth as well as sharp edges at the facets.

2. ECS via Legendre transform of the anisotropic surface free energy

The starting point for an analytic description of portions of the ECS and for discussing the effects of repulsive and attractive step interactions on this shape will be the orientation dependent surface free energy (in one dimension) formulated as follows:

$$f(p) = f_0 + f_1 p + f_3 p^3 + f_4 p^4 + \cdots \tag{1}$$

where p is the step density of the surface, f_0 the surface free energy of the flat terrace (facet), f_1 the free energy of an isolated step, and f_3 and f_4 step interaction energies, respectively [3]. Eq. (1) is generally believed to be valid for an angular range of about 20° but, as we will see further below, it is apparently capable of fitting experimental vicinal shapes at even larger angles. A quadratic term in step density is not considered. This term corresponds to a long-range $1/x$ step interaction pair potential [44,45], for which the total step interaction energy for a vicinal surface would normally diverge [46]. However, a negative f_2 has been found to successfully describe the behavior of a network of crossing steps on some vicinal surfaces [47,48]. By comparison, the physical basis for step interactions of type f_3 and f_4 is well understood [3,49,50].

A portion of the ECS given by $z(x)$, consisting of a facet and adjacent vicinal surface, can be obtained by applying the Legendre transform to $f(p)$ [19,51,52]. We use this transform to generate the shape function $z(x)$ in parameterized form [53]:

$$z = \frac{1}{\lambda}\left(f(p) - p\frac{\mathrm{d}f}{\mathrm{d}p}\right), \quad x = -\frac{1}{\lambda}\frac{\mathrm{d}f}{\mathrm{d}p} \tag{2}$$

where λ is a constant equal to the ratio of facet energy over the separation between the facet and the center of the ECS, $\lambda = f_0/z_0$. For $f_3 > 0$, i.e. repulsive step interaction, a solution for $z(x)$ is [2]

$$\begin{aligned} z(x) &= z_0 - \frac{2}{3}\left(\frac{\lambda}{3f_3}\right)^{1/2}(x - x_0)^{3/2} + \frac{\lambda f_4}{3f_3^2}(x - x_0)^2 \\ &\quad + \cdots, \quad x > x_0, \\ z(x) &= z_0, \quad x < x_0 \end{aligned} \tag{3}$$

with x_0 being the x-coordinate of the facet boundary. For $f_4 = 0$ the second term vanishes, and the shape exhibits a universal shape exponent of 3/2 [2]. If both step interaction terms contribute, there will not be a universal shape exponent but

the effective exponent will vary between 1.5 and 2, depending on the range $x - x_0$ being evaluated.

Note that an equivalent analytical solution is not available for attractive step interactions, $f_3 < 0$. However, the parameterized solution, Eq. (2), is still valid. It is also valid for mixed repulsive/attractive step interactions with $f_3 > 0$, $f_4 < 0$.

3. Repulsive versus attractive step interactions; facet boundary

Applying the formalism of Eq. (2) to Eq. (1) and considering the location of the facet boundary, $x = x_0$, leads to the following simple equation for the coordinate z_0 (with $\lambda = f_0/z_0$):

$$z_0 \equiv z(x_0) = \frac{1}{\lambda}\left(f_0 - 2f_3 p_f^3 - 3f_4 p_f^4\right) = z_0 - \frac{1}{\lambda}\left(2f_3 p_f^3 + 3f_4 p_f^4\right), \quad p(x_0) = p_f \tag{4}$$

We have now a condition for the slope at the facet boundary from Eq. (4), namely $(2f_3 + 3f_4 p_f)p_f^3 = 0$. There are two solutions: either $p_f = 0$ or $(2f_3 + 3f_4 p_f) = 0$ for $p_f \neq 0$. In the first case, for positive values of f_3 and positive or negative f_4, the transition from the facet to the vicinal surface will be smooth, i.e. all orientations will be present on the ECS. Here the Lagrange parameter λ is also equal to f_1/x_0. In the second case, $p_f \neq 0$, there will be a sharp edge at the facet boundary whose contact angle to the facet, θ_f, is given by

$$p_f = \tan\theta_f = -\frac{2f_3}{3f_4}, \quad f_3 < 0 \tag{5}$$

Here f_3 has to be negative and f_4 positive to yield a physically meaningful solution. The contact angle is thus directly dependent on the ratio $|f_3/f_4|$. In the particular case of mixed attractive/repulsive step interactions the position of the facet edge, x_0, no longer corresponds to f_1 but is shifted to smaller values. Equivalently, $\lambda \neq f_1/x_0$. The correct step free energy is then calculated from x_0 and the interaction energies f_3 and f_4, according to (only positive x values):

$$x_0(p_f \neq 0) = \frac{1}{\lambda}\left(f_1 + \frac{4}{27}f_3\left(\frac{f_3}{f_4}\right)^2\right), \quad \lambda = \frac{f_0}{z_0}, \ f_3 < 0$$

or

$$f_1 = \frac{x_0}{z_0}f_0 - \frac{4}{27}f_3\left(\frac{f_3}{f_4}\right)^2 \tag{6}$$

We see from Eqs. (5) and (6) that the larger the ratio of $|f_3/f_4|$, the more the position of the facet edge x_0 will deviate from its "ideal" position f_1/λ and the sharper will be the edge at the facet. In fact, Eq. (5) provides a means of obtaining an estimate of f_3/f_4 from an experimentally measurable facet contact angle. Eq. (6) provides a correlation between the second measurable quantity, i.e. the value of $x_0(p_f \neq 0)$, and the step energy parameters. Then, utilizing the parameterized Eq. (2) for z and x and varying f_1 and f_3 for a fixed ratio f_3/f_4, allows one to fit the experimentally determined shape of the vicinal part of the ECS and thus determine an optimum set of step energetic parameters.

The dependence of a portion of the ECS in the vicinity of a facet is illustrated in Fig. 1 for three conditions discussed above. Choosing $x_0/z_0 = 0.35$, $f_3/f_0 = 0.5$ and $f_4/f_0 = 0.3$ generates the shape shown in Fig. 1a. The facet edge is located at $x = 0.35z_0$ and the transition from the facet to the vicinal surface is continuous, as required for repulsive step interaction, $f_3 > 0$. Changing the sign of f_4/f_0 to -0.3 leads to the shape shown in Fig. 1b which is also continuous. By comparison, for $x_0/z_0 = 0.327$, $f_1/f_0 = 0.35$, $f_3/f_0 = -0.5$ and $f_4/f_0 = 1.0$ the resulting shape is shown in Fig. 1c. The facet edge is now shifted inward and there is a large contact angle of 18.4° at the facet. In general, the facet size (diameter) shrinks for negative f_3, with increasing $|f_3|$ and increasing ratio $|f_3/f_4|$.

4. Examples: shapes and step free energies for Pb and Au ECSs

Experimental investigations of the ECSs of Pb and Au by SEM have demonstrated the principal

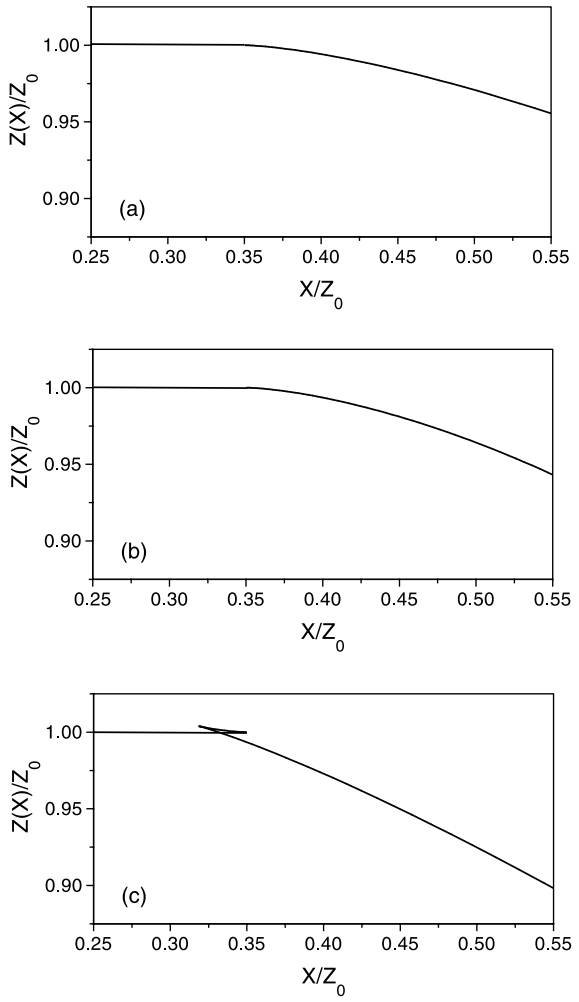

Fig. 1. Plotted sections of calculated profiles, $z(x)/z_0$ versus x/z_0, of the ECS for three different choices of parameters, f_1, f_3 and f_4 (all of them relative to f_0). (a) $f_1 = x_0 = 0.35$, $f_3 = 0.5$, and $f_4 = 0.3$; (b) $f_1 = x_0 = 0.35$, $f_3 = 0.5$, and $f_4 = -0.3$; (c) $x_0 = 0.327$, $f_1 = 0.35$, $f_3 = -0.5$, and $f_4 = 1.0$.

differences of the facet-to-vicinal transition: continuous for Pb [6,54], at least below 577 K [55], and discontinuous for Au [5,9]. In the latter case Au crystallites on two different supports, graphite and α-SiC, have been used to check for a possible influence of support material on the ECS. No significant influence has been found. More recent STM studies of the Pb ECS have essentially confirmed the earlier result [15,16]. Again, a number of different supports have been used for Pb, with essentially identical results, especially concerning the facet-to-vicinal transition.

4.1. Pb equilibrium crystal shape

We present here some recent results obtained for Pb crystallites supported on a Ru(0 0 1) crystal and imaged by STM at temperature. The main emphasis is on the facet-to-vicinal transition and on shape analysis of the curved part next to the facet. Fig. 2a shows an STM image of part of the (1 1 1) facet and adjacent vicinal surface of a Pb crystallite at 383 K. The STM image recorded at the elevated temperature exhibits a series of monoatomic steps all around the stepless (1 1 1) facet. The advantage of step resolved images of the ECS is the fact that the edge of the facet, x_0, can be located precisely, in this case at an average of 265 nm. Steps have a wavy appearance due to fluctuations (except when the scan direction is exactly parallel to the step direction). A portion of a line scan taken for a certain azimuthal direction is presented in Fig. 2b. This scan was successfully fitted with Eq. (3) yielding relative values of $f_3/\lambda = 2065$ nm and $f_4/\lambda = -320$ nm. Alternatively, fitting the data in Fig. 2b with Eq. (3), modified by setting $f_4 = 0$ and by assuming a free exponent n, resulted in $f_3/\lambda = 1840$ nm and $n = 1.48$. The similarity of f_3/λ values obtained in the two fits indicates that the second term of Eq. (3) is not very important in this case, i.e. that the influence of the f_4 interaction is minor. The same kind of fit was carried out for 180 line scans, taken in 2° azimuthal increments all around the (1 1 1) facet. There was considerable scatter in the pre-factor of $(x - x_0)^n$, with average values of f_3/λ and n of 1480 nm and 1.49 ± 0.06, respectively. The average value for the exponent is indeed very close to the theoretically predicted universal value of 1.5, in contrast to a previous report of non-universal behavior [17]. We believe that this difference is due to the present ability to measure the ECS at temperature of 383 K while previously all STM imaging was carried out at room temperature. The scatter in f_3 is quite large because the primary scatter is in the fitted pre-factor which contains f_3 as the inverse square root. To convert x_0 and f_3/λ to actual energies, we estimated the ratio x_0/z_0 to

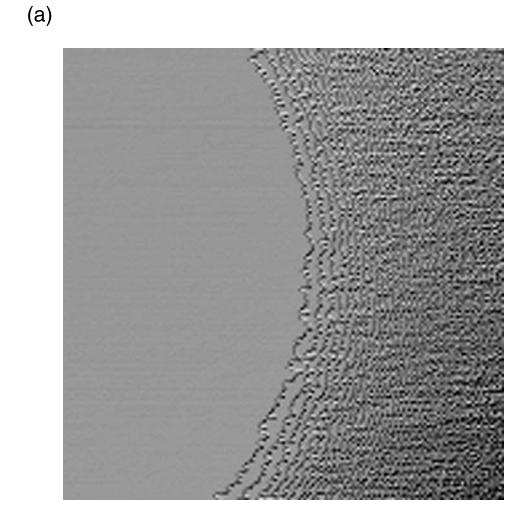

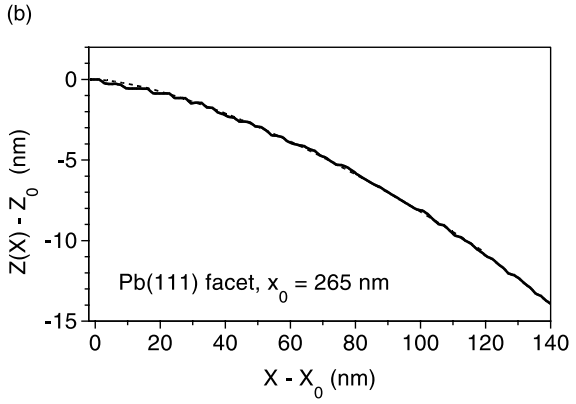

Fig. 2. (a) STM image of a section of the ECS of a Pb crystallite at 383 K. The image shows the facet to vicinal surface transition where the latter is characterized by a train of monatomic steps. (b) Example of a line scan across the ECS in the area of facet to vicinal surface transition. The line scan, $z(x) - z_0$ versus $x - x_0$, normalized relative to the facet edge at z_0, x_0, is fitted by Eq. (3) without the f_4 term.

be equal to 0.22 [17] and assumed $f_0 = 38$ meV/Å^2 [56]. The step free energy f_1 is then equal to 8.37 meV/Å^2 and the step interaction energy assumes a rather large value of $f_3 = 47$ meV/Å^2.

4.2. Au ECS: Effect of surface reconstruction or attractive step interaction?

Next we present in Fig. 3 an example of a cross-sectional ECS image of Au (annealed at 1143 K,

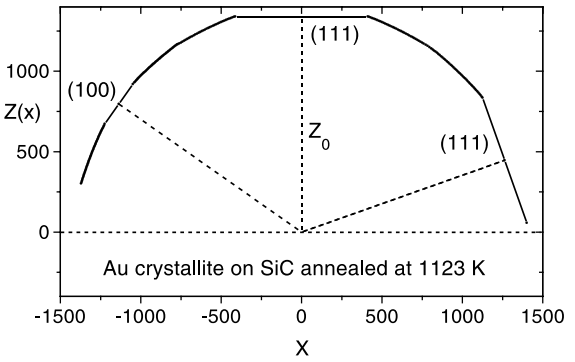

Fig. 3. Cross-section of the ECS of a Au crystallite as imaged by SEM [9]. The temperature of equilibration was 1123 K. (1 1 1) and (1 0 0) facets are clearly visible in this outline of the ECS. The transitions from the facets to the vicinal surfaces are characterized by sharp edges.

crystal radius about 5 μm [9]) taken by SEM. This and other results from Au crystallites, supported on a α-SiC(0 0 1) crystal, had been evaluated previously, assuming a quadratic and a third order term in step density in the surface free energy expression, Eq. (1) [9]. The authors interpreted the sharp edges at the (1 1 1) and (1 0 0) facets in terms of a negative (attractive) step interaction f_2 and a repulsive interaction f_3, without considering f_4. In view of the poorly understood physics of the f_2 term [44,57], we propose to re-evaluate the Au data by using the approach outlined above, based on an attractive f_3 and a repulsive f_4 interaction. Alternatively, the Au ECS vicinal shapes will also be fitted in the framework of a surface reconstruction model to be explained in detail below.

Portions of the ECS in the vicinity of the (1 1 1) and (1 0 0) facets were taken from the data of Fig. 3 and replotted in Fig. 4 after normalizing all lengths, such that the facets are at $z(x)/z_0 = 1$. The experimental data were fitted by $z(x)$ calculated by means of Eqs. (2), (4) and (5). Here we utilized the experimentally accessible radii of the facets and the corresponding contact angles as primary input. These numbers are given in Table 1. Our evaluation of the contact angles yielded 21° and 6° for the (1 1 1) and (1 0 0) edges, respectively, which are somewhat different from those quoted by Wang and Wynblatt [9]. Fitting the experimental data for both sets of contact angles yielded the relative

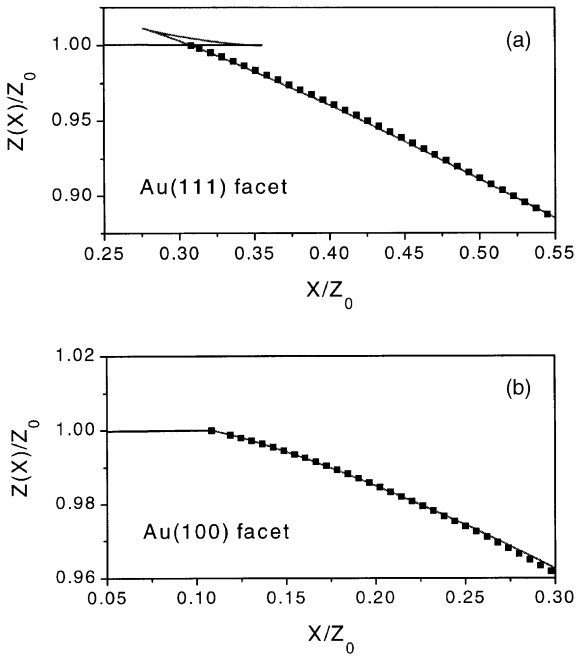

Fig. 4. Portions of the SEM image cross-section of Fig. 3 showing in detail the facet-to-vicinal transitions for (a) the (1 1 1) facet; (b) the (1 0 0) facet. The vicinal portions are fitted by Eq. (3) with f_1 ($f_1 \neq x_0$), an attractive f_3 and repulsive f_4 to match the facet contact angle and the position of the edge. For parameters see Table 1.

energies f_1/f_0, f_3/f_0 and f_4/f_0 which are also summarized in Table 1. The quality of the fit is in all cases very satisfactory, at least for a range of x/z_0 of the order of the facet radius.

For both facets, the evaluated step free energies f_1/f_0 are larger than the corresponding facet edge which is expected for non-regular shapes. The difference is larger for the (1 1 1) facet since the contact angle in that case is considerably larger than the one measured for the (1 0 0) facet. The comparison with the previous evaluation [9] is interesting. Based on the approach of Wang and Wynblatt, the relative f_1/f_0 values were reported as 0.408 and 0.116 for the (1 1 1) and (1 0 0) facet, respectively [9]. Converted to energies, they are 34.2 and 10.1 meV/Å^2 [9], while the present evaluation yields 29.7 and 9.5 meV/Å^2 for steps bounding (1 1 1) and (1 0 0) facets, respectively. The difference for the (1 1 1) vicinal steps amounts thus to 15%.

An alternative approach for explaining a discontinuous facet-to-vicinal transition rests on a difference in surface free energy between a reconstructed facet, e.g. the (1 1 1) facet, and the unreconstructed terraces of the same orientation on the vicinal surfaces. In the case of Au it is well known that both the (1 1 1) and (1 0 0) surfaces are reconstructed [58–61], with large 23×1 and 20×5 unit cells, respectively. The reconstructions are stable over a wide temperature range, such as $T < 685$ and 970 K, respectively [62,63]. On a vicinal surface, terraces are assumed to be unreconstructed, the main reason being their limited size in the direction perpendicular to the bounding steps. In the following we analyze the measured vicinal shapes of the Au ECS in the framework of this reconstruction model [43,64].

At first we fit the curved portion of the ECS next to a facet by Eq. (3), assuming a continuous transition between a fictitious (non-reconstructed) facet and the vicinal surfaces. This requires an offset in $z(x)$ at the facet, equivalent to the surface free energy difference between the reconstructed and unreconstructed facets, Δf_0. Such a fit is shown in Fig. 5 for the (1 1 1) facet and vicinal range while the corresponding energy values are listed in Table 2. We have fitted the experimental data with a combination of f_3 and f_4 and also with f_3 only, the so-called Pokrovsky–Talapov expres-

Table 1
Geometric and relative step energetic parameters to fit facet size and vicinal shape of Au(1 1 1) and (1 0 0) facets

Parameter	(1 1 1) facet, Fig. 4a	(1 1 1) facet [9]	(1 0 0) facet, Fig. 4b	(1 0 0) facet [9]
Facet contact angle θ_f	21°	19.3°	6°	5°
Facet edge x_0/z_0	0.308	0.308	0.108	0.108
Step free energy f_1/f_0	0.354	0.331	0.112	0.110
Step interaction f_3/f_0	−0.950	−0.573	−1.025	−0.722
Step interaction f_4/f_0	1.65	1.09	6.50	5.50

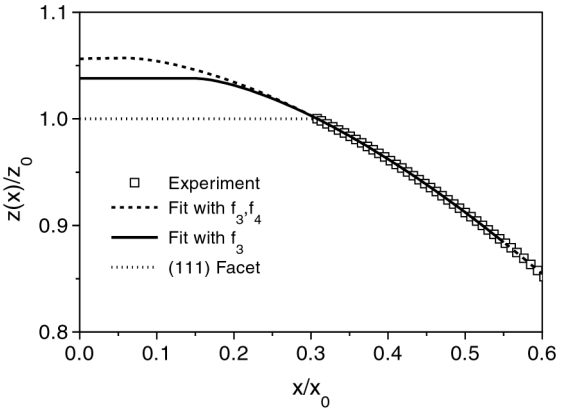

Fig. 5. Similar to Fig. 4a, but fitted by Eq. (3) allowing for a continuous facet-to-vicinal transition where the facet now represents the unreconstructed case. Hence its free energy is larger than that of the reconstructed one (located at $z/z_0 = 1$).

sion (only the first term of Eq. (3)). Excellent fits were obtained in both cases, for the (1 1 1) as well as the (1 0 0) vicinity. It is obvious from Fig. 5 and the position of the facet edge for the unreconstructed facet that the step free energy is now much smaller than the experimental x_0 defined by the position of the sharp edge. This value of the step free energy, however, is representative of steps in contact with the unreconstructed facet. The step free energy of steps bounding the reconstructed facet remains undetermined but an estimate will be given below.

A similar situation to that in Fig. 5 exists for the (1 0 0) vicinal range. The difference in Δf_0 is much smaller than for the (1 1 1) vicinal surface because the contact angle is only 6° compared to 20° for the (1 1 1). The contact angles were calculated from the ratios of $\Delta f_0/f_0$, f_3/f_0 and f_4/f_0 obtained by the curve fitting process, according to the implicit relationship [64] extended to include both step interactions f_3 and f_4:

$$p_f = \tan\theta_f = \left(\frac{\Delta f_0}{2f_3 + 3f_4 p_f}\right)^{1/3} \tag{7}$$

inserting the energies found by curve fitting yields contact angles of 19–20° and 5.5–6.5° for the (1 1 1) and (1 0 0) facets, respectively (Table 2).

Since the evaluated f_1 is representative of the unreconstructed facet case, we can try and estimate the step free energy of the reconstructed case according to the simple relationship, $f_{1r} - f_{1u} = (f_{0u} - f_{0r})/p_c$, where p_c is the step density at the crossing of the two surface free energy functions, $f_r(p)$ and $f_u(p)$, of the reconstructed (r) and unreconstructed (u) case, with the step interaction energies assumed to be the same for both [65]. Assuming further that this crossing occurs at midway between zero and p_f, the step free energy of the reconstructed facet-to-vicinal transition is obtained from this formula by setting $p_c = p_f/2$. The result is added in Table 2 and the ratios of the (1 1 1) to (1 0 0) step free energies f_{1r} are in the range 2.8–3.0, quite close to the value of 3.1, which was obtained for the mixed attractive/repulsive step interaction model.

Table 2
Step-related free energies in meV/Å^2, evaluated from vicinal Au(1 1 1) and (1 0 0) surfaces, according to the (1 1 1) facet reconstruction model and the attractive/repulsive step–step interaction model

	(1 1 1) vicinal			(1 0 0) vicinal		
	Reconstructed facet		1 × 1 facet	Reconstructed facet		1 × 1 facet
	PT (only repulsive f_3)	f_3 repulsive, f_4 open	f_3 attractive, f_4 repulsive	PT (only repulsive f_3)	f_3 repulsive, f_4 open	f_3 attractive, f_4 repulsive
f_0 [9]	83.75	83.75	83.75	86.63	86.63	86.63
f_{1u}; f_{1r}	12.7; 30.2	5.2; 32.9	29.6	5.8; 10.7	6.9; 11.0	9.5
f_3	33	92	−80	92	67	−89
f_4	–	−61	138	–	14	563
$\Delta f_0/f_0$	0.038	0.057	–	0.0032	0.0020	–
θ_{facet}	20°	19°	21°	6.5°	5.5°	6°
$f_{1r}(1\,1\,1)/f_{1r}(1\,0\,0)$	2.8	3.0	3.1			

PT: Pokrovsky–Talapov shape with exponent 3/2.

The absolute step free energies coming out of the two models are quite similar, of the order of 30 meV/Å^2 for the (1 1 1) vicinal surface and 10 meV/Å^2 for the (1 0 0) vicinal surface. Theoretical values of the step free energy for (unreconstructed) Au(1 1 1) vicinals range between 21 meV/Å^2 [66] and 70 meV/Å^2 [67] while the step energy ratio for (1 1 1) to (1 0 0) vicinal surfaces has been reported as 2.5 [66] and 3.2 [67]. Similar ratios of about 3 have also been obtained theoretically for corresponding Ag and Pt vicinal surfaces [68]. Hence the agreement for the step energy ratio is reasonable. Based on an empirical correlation between surface and step free energies for fcc (1 1 1) vicinal surfaces [69], one estimates for the (1 1 1) vicinal of Au a step free energy of 32 meV/Å^2, according to 37% of the average surface free energy of 87.5 meV/Å^2 [70]. The value of 32 meV/Å^2 is close to the present result of 30 meV/Å^2.

5. Discussion

From the current data for Pb and Au ECSs and their evaluation it seems obvious that the results for Pb are fairly consistent with the theory of vicinal shapes in contact with unreconstructed facets. The transition is continuous on a microscopic scale (provided we average over monatomic steps), the curvature is well described by repulsive step–step interactions, and the critical exponent is close to the theoretical value of 3/2, in support of a step interaction potential proportional to $1/x^2$ [3,49]. On the other hand, for Au we have the interesting situation that two different theoretical models seem to be equally well applicable to a quantitative description of sharp edges at the (1 1 1) and (1 0 0) facets of the Au ECS. Hence we will try to find some arguments for giving a priority to one of the models.

In their seminal paper on the physics of step–step interactions and their role in governing the facet-to-vicinal transition Jayaprakash et al. [3] point out the three major physical sources of step interactions. These are due to kink formation and step fluctuations, the so-called entropic interaction [49], elastic interaction due to dipole [50,71] and higher order dipole–quadrupole interactions [46], and electric dipole interaction, associated with intrinsic step dipoles [72,73] or dipole moments associated with step-adsorbed atoms or molecules [3]. All of these interactions, except those due to force quadrupoles, are long range and vary as $\sim 1/x^2$, i.e. they contribute to the $f_3 p^3$ term of Eq. (1). Entropic step interactions are strongly temperature dependent while elastic and electric dipole interactions are not. Entropic and elastic interactions are generally repulsive while electric dipole interactions can be repulsive or attractive, depending on the orientation of the dipole relative to the surface [3]. If the dipole moment is equal to $\vec{\pi} = \vec{\pi}_\perp + \vec{\pi}_\parallel$ where $\vec{\pi}_\parallel$ is parallel to the surface and normal to the step direction, and $\vec{\pi}_\perp$ perpendicular to both the step and the surface, then the step interaction is proportional to $(\vec{\pi}_\perp^2 - \vec{\pi}_\parallel^2)p^3$. This difference can be negative such that an attractive contribution results. The overall step interaction may then be attractive if the electric dipole interaction dominates the elastic and entropic interactions which is more likely at low temperatures. Thus there is, in principle, a mechanism for attractive step interaction.

The fourth order term $f_4 p^4$ (and also a fifth order term) has its origin in force quadrupoles at the step interacting with force dipoles [46] and possibly in equivalent electric quadrupole interactions. Model calculations of elastic step interactions have demonstrated the necessity of higher order terms. In these calculations f_4 (and f_5) turned out to be negative for (1 0 0) vicinals of a number of fcc metals, Au being one of them. However there is no reason, in principle, why f_4 could not be positive if f_3 is negative. These cases have not been considered thus far.

It seems reasonable, therefore, to consider step–step interactions proportional to $1/x^2$ to be the major contribution to the orientation dependent surface free energy, rather than a long-range $1/x$ interaction, that was proposed to be associated with electronic surface state-mediated interactions [44,57], although the exact form of the interaction potential for this type of step interaction seems to be a matter of debate [45]. It is also not clear whether this interaction can be attractive or should be strictly repulsive. Because of this general uncertainty we believe that the present approach of

assuming the step interaction f_3 to be the most important and either repulsive or attractive, depending on the type of material, is physically sound. The step free energies and step interaction energies evaluated from the ECS on this basis are probably closer to reality than those obtained by the previous approach [9]. Since we derive numbers for f_3 and f_4 from the experimental Au ECS, we can construct the step–step interaction potential for vicinal (1 1 1) and (1 0 0) surfaces. If the potential is given by $V_{s-s}(x) = A_2p^2 + A_3p^3$, where x is the separation between steps and $p = h/x \cong \tan\theta$ for small angles, the constants A_2, A_3 are given by the relative step interaction energies listed in Table 1. A plot of $V_{s-s}(x)$ versus h/x, shown in Fig. 6, exhibits clear minima at 4.35° and 15.6° for (1 0 0) and (1 1 1) vicinals, respectively, favoring stable facets near those orientations.

Fitting the vicinal shapes near (1 1 1) and (1 0 0) facets of the ECS of Au within the reconstruction model yields even more quantitative energy data than the mixed step interaction model and is thus possibly more vulnerable for a critical examination of such data. In particular, there are values of surface and step free energies for the reconstructed and unreconstructed facet orientations, summarized in Table 2, which may be compared to relevant theory or experiment. The differences in surface free energies between the reconstructed and unreconstructed facets, $\Delta f_0/f_0$, were evaluated as 3.8–5.7% and 0.2–0.3% for the (1 1 1) and (1 0 0) facets, respectively. They are both small, as expected, but they appear to be in the wrong order, i.e. the larger difference is obtained for the (1 1 1) facet. Here the reconstruction consists essentially of a close-packed monolayer of Au on a close-packed (1 1 1) surface, with a 4.2% denser packing in the upper layer. For the less dense (1 0 0) surface, on the other hand, a similar compressed close-packed layer is epitaxial to this (1 0 0) surface. Thus the larger crystallographic misfit between the first and second layer for the (1 0 0) surface is reason to expect a larger difference in $\Delta f_0/f_0$. This is indeed found theoretically by a large change in $\Delta f_0/f_0$ of about 15–20% for the (1 0 0) orientation [32,74]. By comparison, the corresponding change for the (1 1 1) orientation was reported as 6.6% [74]. There are no direct experimental surface free energy data to compare with. However, the reconstructed and unreconstructed Au(1 1 1) and Au(1 0 0) surfaces have been prepared and characterized electrochemically by their zero-charge potentials which are a measure of the work function of the surface [75]. The differences are 0.22 and 0.09 V for the (1 0 0) and (1 1 1) surfaces, indirectly indicative of a smaller surface free energy difference in the case of (1 1 1). Hence there is clearly an inconsistency in the order of $\Delta f_0/f_0$ for Au(1 1 1) and (1 0 0), evaluated from the experimental ECS data of Au [4,9].

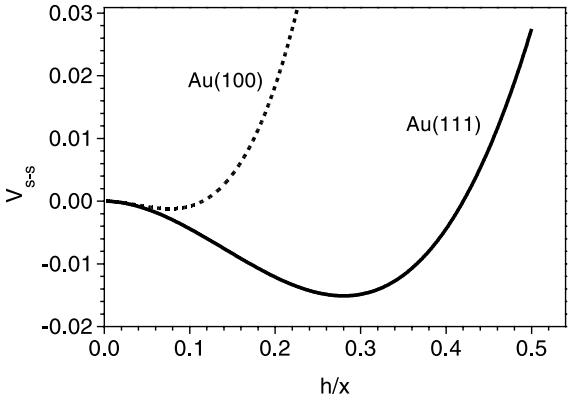

Fig. 6. Plot of step–step interaction potential versus h/x for steps on vicinal Au(1 1 1) and (1 0 0) surfaces, according to the step interaction energies in Table 1.

A similar inconsistency is obtained in the analysis of step free energies of the reconstructed and unreconstructed Au(1 1 1) and (1 0 0) surfaces. This is no surprise since we have a direct proportionality between $\Delta f_0/f_0$ and the difference in step free energies, $f_{1r} - f_{1u}$. The latter are not only unreasonably large but most likely also in the wrong order. A particularly severe problem exists for Au(1 1 1). In fact, the theoretical values of the step free energy of Au(1 1 1) vicinals quoted above were all obtained for unreconstructed surfaces [66,67]. Hence they should be compared with f_{1u} and not f_{1r}, revealing a large discrepancy between experiment and theory. For Au(1 0 0), on the other hand, the situation is less severe since the differences in f_{1r} and f_{1u} and $\Delta f_0/f_0$ are small. Clearly, the energy data evaluated with the reconstruction model for the Au(1 1 1) vicinal surfaces are

inconsistent. The possible origin of this inconsistency could be, for example, the high temperature of equilibration and/or the accuracy of the facet contact angle determination by SEM, here for the (1 1 1) facet in particular. Both experimental issues will be discussed in the following.

At first let us have a critical look at the reported large contact angle of 20° at the (1 1 1) facet of Au [4,5,9]. How reliable is this contact angle evaluated from scanning electron microscope images? SEM has a resolution of about 10–30 nm and it is conceivable that small facets next to the (1 1 1), having lower contact angles, were not resolved. To shed light on this issue, we compare the results of unstable flat and modulated vicinal surfaces of Au(1 1 1) and (1 0 0) with the reported sharp edges on the Au ECS. For (1 0 0) vicinals the range of instability was about 7–8° [23,29,36] whereas for (1 1 1) vicinals several stable facet-like features were reported at 4°, 7° and 12° depending on azimuth [23,24,28,37]. So there is rough agreement with the 6.5° at the (1 0 0) facet but we notice a serious discrepancy for the (1 1 1) orientation, because a range of 20° of unstable orientations next to the (1 1 1) facet finds no support from these investigations. If a narrow facet with a contact angle of 4° or 7° would exist on the ECS in the vicinity of the (1 1 1) facet, the evaluated differences in surface and step free energies would be significantly smaller and thus more consistent with the edge at the (1 0 0) facet and other experiments and theory. This situation calls for better resolved images of the Au ECS, especially in the vicinity of (1 1 1) facets.

On the other hand, if the 20° contact angle at the (1 1 1) facet of the Au ECS should be confirmed by future experiments, e.g. by an STM investigation, the observed serious inconsistency resulting from the evaluation in terms of the surface reconstruction model would disqualify this model for explaining the discontinuous facet-to-vicinal transition. In that case the model based on mixed attractive/repulsive step interactions should be the preferred choice although the physical detail of strong step–step attractive forces would have to be studied.

The second point of concern is that the ECSs of Au had been equilibrated at very high temperatures, such as 1273 K [4] and 1123 K [9]. These are well above the disordering temperature of the (1 1 1) and (1 0 0) surface of Au. The temperature dependence of reconstruction of Au(1 1 1) and (1 0 0) has been studied and it was found that an order–disorder transition occurs at 685 and 970 K, respectively [62,63]. However, despite the disorder the Au(1 1 1) is still reconstructed even at 1225 K, with the top layer present as an incommensurate compressed fluid phase [28]. Hence one cannot argue that reconstruction does not play any role for crystallites equilibrated at such a high temperature. Furthermore, the crystallites were imaged by SEM at room temperature, such that changes of facet structure and vicinal shape could have occurred during cooling. A significant change of the facet contact angles during cooling, on the other hand, is hardly conceivable. This issue is difficult to resolve unless the ECS is imaged at the temperature of equilibration.

Lastly, let us briefly discuss the value of obtaining relative step free energies (and step interaction energies) from the 3D ECS of crystallites. Of course, the primary data are shapes and length ratios, such as a ratio of step to surface free energy. An experimental (or theoretical) value of the average surface free energy is usually chosen to obtain an *absolute* step free energy from the ECS. Hence any step free energy obtained in this way is only as reliable as the surface free energy input. For this reason the degree of uncertainty of step free energies determined in this fashion is relatively high. A comparison of these experimental step free energies, based on the ECS, with theoretical values can be quite unsatisfactory, in particular, if there is a large spread in the latter. Obviously this is the case for Au. One way out of this dilemma is the experimental determination of the *absolute* step free energy, either from temperature dependent 2D island shapes and step fluctuations [76–78] or by measuring the variation of the facet size on the 3D ECS as a function of temperature [79]. The latter technique has the added advantage of providing an *absolute* value of the surface free energy and its anisotropy. However, an application of this technique and its comparison with the other two is still lacking. Having three independent experimental techniques to determine the absolute step free

energy for a particular step orientation should provide a sound basis for removing some of the ambiguities in currently known values of this important quantity in surface physics.

Acknowledgements

We gratefully acknowledge an ongoing discussion on surface energetics with Harald Ibach and his constructive comments on this manuscript. This work was supported in part by the NSF-MRSEC at UMD (DMR-00-80008).

References

[1] C. Rottman, M. Wortis, Phys. Rev. B 29 (1984) 328.
[2] C. Jayaprakash, W.F. Saam, Phys. Rev. B 30 (1984) 3916.
[3] C. Jayaprakash, C. Rottman, W.F. Saam, Phys. Rev. B 30 (1984) 6549.
[4] J.C. Heyraud, J.J. Métois, Acta Metall. 28 (1980) 1789.
[5] J.C. Heyraud, J.J. Métois, J. Crystal Growth 50 (1980) 571.
[6] J.C. Heyraud, J.J. Métois, Surf. Sci. 128 (1983) 334.
[7] J.C. Heyraud, J.J. Métois, Surf. Sci. 180 (1987) 647.
[8] A. Pavlovska, D. Dobrev, E. Bauer, Surf. Sci. 326 (1995) 101.
[9] Z. Wang, P. Wynblatt, Surf. Sci. 398 (1998) 259.
[10] W.C. Cheng, P. Wynblatt, Surf. Sci. 302 (1994) 179.
[11] W.C. Cheng, P. Wynblatt, Surf. Sci. 302 (1994) 185.
[12] C.R. Henry, Surf. Sci. Rep. 31 (1998) 231.
[13] G. Rao, D.B. Zhang, P. Wynblatt, Acta Metall. Mater. 41 (1993) 3331.
[14] S. Surnev, P. Coenen, B. Voigtländer, H.P. Bonzel, P. Wynblatt, Phys. Rev. B 56 (1997) 12131.
[15] S. Surnev, K. Arenhold, P. Coenen, B. Voigtländer, H.P. Bonzel, P. Wynblatt, J. Vac. Sci. Technol. A 16 (1998) 1059.
[16] K. Arenhold, S. Surnev, P. Coenen, H.P. Bonzel, P. Wynblatt, Surf. Sci. 417 (1998) L1160.
[17] K. Arenhold, S. Surnev, H.P. Bonzel, P. Wynblatt, Surf. Sci. 424 (1999) 271.
[18] K.H. Hansen, T. Worren, S. Stempel, E. Laegsgaard, M. Bäumer, H.J. Freund, F. Besenbacher, I. Stensgaard, Phys. Rev. Lett. 83 (1999) 4120.
[19] A.F. Andreev, Zh. Eksp. Teor. Fiz. 80 (1981) 2042.
[20] W.K. Burton, N. Cabrera, Disc. Faraday Soc. 5 (1949) 33.
[21] W.K. Burton, N. Cabrera, F.C. Frank, Trans. Royal Soc. London A 243 (1951) 299.
[22] U. Breuer, H.P. Bonzel, Surf. Sci. 273 (1992) 219.
[23] H.P. Bonzel, U. Breuer, B. Voigtländer, E. Zeldov, Surf. Sci. 272 (1992) 10.
[24] M. Salmeron, D.S. Kaufman, B. Marchon, S. Ferrer, Appl. Surf. Sci. 28 (1987) 279.
[25] D. Gibbs, B.M. Ocko, D.M. Zehner, S.G.J. Mochrie, Phys. Rev. B 38 (1988) 7303.
[26] Y. Samson, S. Rousset, S. Gauthier, J.C. Girard, J. Klein, Surf. Sci. 315 (1994) L969.
[27] F. Pourmir, S. Rousset, S. Gauthier, M. Sotto, J. Klein, L. Lecoeur, J.P. Bellier, Surf. Sci. 324 (1995) L337.
[28] G.M. Watson, D. Gibbs, S. Song, A.R. Sandy, S.G.J. Mochrie, D.M. Zehner, Phys. Rev. B 52 (1995) 12329.
[29] A. Bartolini, F. Ercolessi, E. Tosatti, Phys. Rev. Lett. 63 (1989) 872.
[30] G. Bilalbegovic, F. Ercolessi, E. Tosatti, Europhys. Lett. 18 (1992) 163.
[31] J. Frohn, M. Giesen, M. Poensgen, J.F. Wolf, H. Ibach, Phys. Rev. Lett. 67 (1991) 3543.
[32] D. Tománek, Phys. Lett. 113A (1986) 445.
[33] F. Ercolessi, E. Tosatti, M. Parinello, Phys. Rev. Lett. 57 (1986) 719.
[34] R.J. Phaneuf, E.D. Williams, N.C. Bartelt, Phys. Rev. B 38 (1988) 1984.
[35] W.J. Kaiser, R.C. Jaklevic, Surf. Sci. 181 (1987) 55.
[36] M. Sotto, J.C. Bouillard, Surf. Sci. 214 (1989) 97.
[37] S. Rousset, F. Pourmir, J.M. Berroir, J. Klein, J. Lecoeur, P. Hecquet, B. Salanon, Surf. Sci. 422 (1999) 33.
[38] G.M. Watson, D. Gibbs, D.M. Zehner, M. Yoon, S.G.J. Mochrie, Phys. Rev. Lett. 71 (1993) 3166.
[39] M. Yoon, S.G.J. Mochrie, D.M. Zehner, G.M. Watson, D. Gibbs, Phys. Rev. B 49 (1994) 16702.
[40] M. Yoon, S.G.J. Mochrie, D.M. Zehner, G.M. Watson, D. Gibbs, Surf. Sci. 338 (1995) 225.
[41] R.Q. Hwang, E.D. Williams, R.L. Park, Phys. Rev. B 40 (1989) 11716.
[42] E.D. Williams, N.C. Bartelt, Science 251 (1991) 393.
[43] E.D. Williams, N.C. Bartelt, Ultramicroscopy 31 (1989) 36.
[44] N. Garcia, P.A. Serena, Surf. Sci. 330 (1995) L665.
[45] E. Carlon, Doctoral Thesis, University of Utrecht, 1996.
[46] R. Najafabadi, D. Srolovitz, Surf. Sci. 317 (1994) 221.
[47] E. Carlon, H. van Beijeren, Phys. Rev. Lett. 76 (1996) 4191.
[48] E. Carlon, H. van Beijeren, Phys. Rev. E 62 (2000) 7646.
[49] E.F. Gruber, W.W. Mullins, J. Phys. Chem. Solids 28 (1967) 875.
[50] V.I. Marchenko, A.Y. Parshin, Zh. Eksp. Teor. Fiz. 79 (1980) 257.
[51] N. Cabrera, Surf. Sci. 2 (1964) 320.
[52] L.D. Landau, E.M. Lifshitz, Statistical Physics, vol. V, Addison-Wesley, Reading, 1958, p. 460.
[53] H. van Beijeren, I. Nolden, The Roughening Transition, Topics in Current Physics, vol. 43, Springer, Berlin, 1987, p. 259.
[54] C. Rottman, M. Wortis, J.C. Heyraud, J.J. Métois, Phys. Rev. Lett. 52 (1984) 1009.
[55] J.C. Heyraud, J.J. Métois, J.M. Bermond, J. Cryst. Growth 98 (1989) 355.
[56] A.R. Miedema, J.W.F. Dorleijn, Surf. Sci. 95 (1980) 447.
[57] J.J. Sáenz, N. García, Surf. Sci. 155 (1985) 24.
[58] D.G. Fedak, N.A. Gjostein, Phys. Rev. Lett. 16 (1966) 171.

[59] D.G. Fedak, N.A. Gjostein, Surf. Sci. 8 (1967) 77.
[60] J. Perdereau, J.P. Biberian, G.E. Rhead, J. Phys. Fr. 4 (1974) 1978.
[61] H. Melle, E. Menzel, Z. Naturforsch. A 33 (1978) 282.
[62] K.G. Huang, D. Gibbs, D.M. Zehner, A.R. Sandy, S.G.J. Mochrie, Phys. Rev. Lett. 65 (1990) 3313.
[63] S.G.J. Mochrie, D.M. Zehner, B.M. Ocko, D. Gibbs, Phys. Rev. Lett. 69 (1990) 2925.
[64] N.C. Bartelt, E.D. Williams, R.J. Phaneuf, Y. Yang, S. DasSarma, J. Vac. Sci. Technol. A 7 (1989) 1898.
[65] H.-C. Jeong, E.D. Williams, Surf. Sci. Rep. 34 (1999) 171–294.
[66] P. Stoltze, J. Phys.: Cond. Matter 6 (1994) 9495.
[67] L. Vitos, H.L. Skriver, J. Kollár, Surf. Sci. 425 (1999) 212.
[68] S.V. Khare, T.L. Einstein, Surf. Sci. 314 (1994) L857.
[69] H.P. Bonzel, Surf. Sci. 328 (1995) L571.
[70] V.K. Kumikov, K.B. Khokonov, J. Appl. Phys. 54 (1983) 1346.
[71] L.E. Shilkrot, D.J. Srolovitz, Phys. Rev. B 53 (1996) 11120.
[72] B. Krahl-Urban, E.A. Niekisch, H. Wagner, Surf. Sci. 64 (1977) 52.
[73] K. Besocke, B. Krahl-Urban, H. Wagner, Surf. Sci. 68 (1977) 39.
[74] F. Ercolessi, A. Bartolini, M. Garofalo, M. Parinello, E. Tosatti, Surf. Sci. 189/190 (1987) 636.
[75] D.M. Kolb, J. Schneider, Electrochim. Acta 31 (1986) 929.
[76] D.C. Schlösser, L.K. Verheij, G. Rosenfeld, G. Comsa, Phys. Rev. Lett. 82 (1999) 3843.
[77] G. Schulze Icking-Konert, M. Giesen, H. Ibach, Phys. Rev. Lett. 83 (1999) 3880.
[78] M. Giesen, C. Steimer, H. Ibach, Surf. Sci. 471 (2001) 80.
[79] H.P. Bonzel, A. Emundts, Phys. Rev. Lett. 84 (2000) 5804.